



## Transient liquid phase bonding of Al 2024 to Ti–6Al–4V alloy using Cu–Zn interlayer

Majid SAMAVATIAN<sup>1</sup>, Ayoub HALVAEE<sup>2</sup>, Ahmad Ali AMADEH<sup>2</sup>, Alireza KHODABANDEH<sup>1</sup>

1. Department of Materials Engineering, Tehran Science and Research Branch,  
Islamic Azad University, Tehran 50122, Iran;

2. School of Metallurgy and Materials Engineering, University of Tehran, Tehran 50122, Iran

Received 30 May 2014; accepted 14 October 2014

**Abstract:** Transient liquid phase bonding of two dissimilar alloys Al 2024 and Ti–6Al–4V using Cu–22%Zn interlayer was carried out at 510 °C under vacuum of 0.01 Pa for various bonding time. In order to characterize the microstructure evolution in the joint zone, scanning electron microscopy (SEM), energy dispersive spectroscopy (EDS) and X-ray diffraction (XRD) were applied. The results show that joint formation is attributed to the solid-state diffusion of Cu and Zn into Ti–6Al–4V and Al 2024 alloys followed by eutectic formation and isothermal solidification along the Cu–Zn/Al 2024 interface. The hardness of the joints at the interface increases with an increase in bonding time which can be attributed to formation of intermetallic compounds such as Al<sub>2</sub>Cu, TiCu<sub>3</sub>, Al<sub>4.2</sub>Cu<sub>3.2</sub>Zn<sub>0.7</sub>, Al<sub>0.71</sub>Zn<sub>0.29</sub>, Ti<sub>2</sub>Cu, TiAl<sub>3</sub> and TiZn<sub>16</sub> in the joint zone. Moreover, shear strength of the joint reaches the highest value of 37 MPa at bonding time of 60 min.

**Key words:** aluminum alloy; transient liquid phase bonding; homogenization; diffusion; intermetallic compound; eutectic

### 1 Introduction

The joining of Al and Ti alloys is desirable to construct hybrid structures in aerospace [1] and automobile [2] industries. The differences in melting temperature and crystal structure create a great challenge to bond Al and Ti dissimilar alloys using traditional fusion welding techniques [3]. On the other hand, the formation of intermetallic compounds such as TiAl and TiAl<sub>3</sub> in the joint zone is a major trouble [4]. These intermetallics are described by their low mechanical properties such as high brittleness and low fracture toughness [5]. For this reason, they lead to a severe decrease in mechanical properties of the joint. To solve this problem, many researchers have proposed various methods like GTA welding–brazing [6,7], laser welding–brazing [8,9], friction stir welding [10], solid-state diffusion bonding [11,12] and TLP bonding [13,14] to make a sound joint. Existence of oxide film on the bonding surfaces impedes the solid-state diffusion bonding of Al alloys [15], while TLP bonding process is highly tolerant to the presence of surface oxide film [16]. Moreover, uncontrollable

formation of TiAl and TiAl<sub>3</sub> intermetallics caused by direct contact of Al and Ti in the solid-state diffusion bonding is a main problem. When an interlayer is placed between the two alloys, it would be claimed that the formation of these intermetallic compounds is controllable.

TLP bonding of Al alloy to Ti–6Al–4V alloy with pure Cu interlayer was formerly done by ALHAZAA et al [17]. Their results show that the maximum shear strength of joint zone is not desired. This might be due to the limitation dissolution zone within Al alloy coupled with lack of diversity in the formation of intermetallics at the interface. Considering this fact, using Cu–Zn interlayer can decrease the eutectic temperature and extend dissolution at the interface. In addition, the creation of more eutectic phases from Al, Cu and Zn is expected in the joint zone.

The joining of Al 2024 alloy to Ti–6Al–4V alloy has not been already attempted by TLP bonding. Hence, this method suggests distinct results in comparison with solid-state joining methods. In this work, we explore the possibility of eutectic formation in the joint zone and characterize the mechanical properties as a function of bonding time.

## 2 Experimental

A Cu–22%Zn foil with the thickness of 50  $\mu\text{m}$  was employed as an interlayer to join Al 2024 alloy to Ti–6Al–4V alloy. The accurate chemical composition of base metals is listed in Table 1.

**Table 1** Chemical compositions of base alloys

Alloy	Mass fraction/%								
	Cu	V	Mg	Fe	Si	Zn	Other	Al	Ti
Al 2024	4.89	0	1.99	0.34	0.25	0.1	<0.1	Bal.	0.03
Ti–6Al–4V	0	4.05	0	0.03	0	0	<0.3	6.1	Bal.

At first, the base metals were cut into dimensions of 10 mm×10 mm×5 mm and the surfaces of samples were prepared by using several stages of grinding papers up to 1200 grit. In order to prevent oxidation of the bond surface, the samples were cleaned ultrasonically using acetone and then immediately placed in ethanol.

The interlayer was kept between the alloys and a fixture was then applied for a uniaxial pressure of 1 MPa onto the samples. The bonding process was performed in a furnace under the vacuum of 0.01 Pa at 510 °C with a heating rate of 70 °C/min. The bonding process was also performed for different bonding time from 20 min up to 60 min. Although the bonding time of 10 min was tested, it did not work because it is probably caused by insufficient diffusion of interlayer into the base alloys. The cross-section of the bonded samples was then polished and etched by Keller's reagent (5 mL HNO<sub>3</sub> + 3 mL HCl + 2 mL HF + 90 mL distilled water) for microscopic evaluation [18]. In order to characterize the joints and identify intermetallic compounds, scanning electron microscopy (SEM), electron dispersive spectroscopy (EDS) and X-ray diffraction (XRD) were applied. The shear strength of specimens was measured according to ASTM standard D1002–99 [19] by MTS30/MH tensile testing machine at a cross-head speed of 0.5 mm/min. Three samples were examined for each parameter. Finally, hardness measurements were conducted by using Mitutoyo HM tester with a load of 50 g.

## 3 Results and discussion

### 3.1 Microstructure and compositional changes

It is believed that the formation of a metallurgical bond for Al 2024 and Ti–6Al–4V alloys using Cu–Zn interlayer depends on two mechanisms. Solid-state diffusion occurs at the Ti alloy interface, while the diffusion of Cu and Zn takes place followed by eutectic liquid formation at the Al alloy interface. The mechanism of bonding process is similar to close systems studied by

ATIEH and KHAN [20,21]. Considering ternary phase diagram of Al–Cu–Zn [22,23], there are phase transformations at 407 and 422 °C that can provide the liquid along the Al alloy interface. Dissolution and widening zone in the transient liquid phase bonding is clearly observed for the bond made at 20 min (see Fig. 1). This zone is separated to three distinct areas within Al 2024 interface marked as *A*, *B* and *C*. According to the EDS analysis (Table 2) and phase diagram for Al–Cu–Zn system, it could be predicted that the intermetallics formed by the diffusion of interlayer into the Al alloy. The chemical composition of 83.26% Al, 12.5% Zn and 3.7% Cu (mass fraction) in area *A* indicates the formation of  $\alpha(\text{Al})$  and  $\tau(\text{Al}_4\text{Cu}_3\text{Zn})$  phases from a phase transformation at 422 °C. It should be noted that the formation of ternary intermetallic is verified by the XRD analysis. In area *B*, Al and Zn contents decrease sensibly compared with that in area *A*, but Cu content increases to 43.01% (mass fraction). Formation of  $\eta$  and  $\tau$  phases that are rich in Cu could be expected in this area. The EDS analysis shows that area *C* mainly consists of 46.43% Al, 1.30% Zn and 51.77% Cu (mass fraction). Considering chemical composition and ternary phase diagram [22],  $\eta$  and  $\theta$  phases are expected to form in this area. It is observed from Fig. 1 that the width of dissolution zone is more than 100  $\mu\text{m}$ , while that for Al/Ti couple bond using pure Cu by ALHAZAA et al [17] is much lower. This can be attributed to the existence of more eutectic formation below 510 °C when Cu–Zn interlayer is applied. In this condition, more liquid is created along the Al 2024 interface.

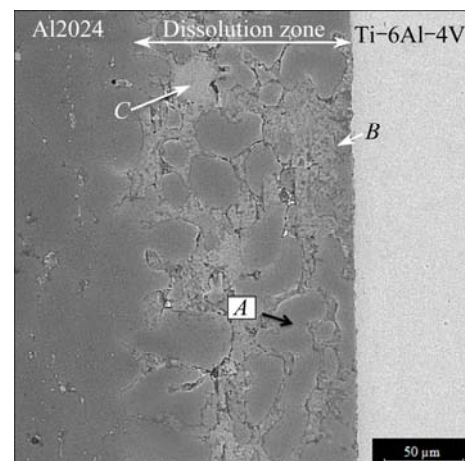


**Fig. 1** SEM image of bond made at 510 °C for 20 min

**Table 2** EDS analysis of different areas in Fig. 1

Area	Mass fraction/%				
	Al	Cu	Zn	Ti	Mg
<i>A</i>	83.26	3.7	12.5	0.1	0.43
<i>B</i>	53.16	43.01	3.10	0.57	0.17
<i>C</i>	46.43	51.77	1.30	0.24	0.26

Figure 2 shows SEM micrograph of a bond made at 40 min. Clearly, with an increase in bonding time, dissolution and widening stage is completed and only sporadic regions remain along the joint zone. Table 3 represents EDS analysis of selected regions in Fig. 2. Area *A* is located parallel to the interface. This area mainly consists of Al and Cu and has a small amount of Fe. Area *B* includes several elements like Al, Cu, Ti, Si and Zn. The presence of these elements suggests the formation of various intermetallics at the interface. Regarding Fig. 2, area *D* encompasses area *C*. According to the chemical analysis, although elements in these two areas are similar, the difference is the amount of these elements. Al, Cu, Fe and Mn contents in area *C* are 69.75%, 6.02%, 13.42% and 9.95%, respectively, while Cu content significantly goes up to 37.97% and Al, Fe and Mn contents decrease in area *D*. This indicates that Cu is set back from area *C* to its environs and forms a distinct phase.

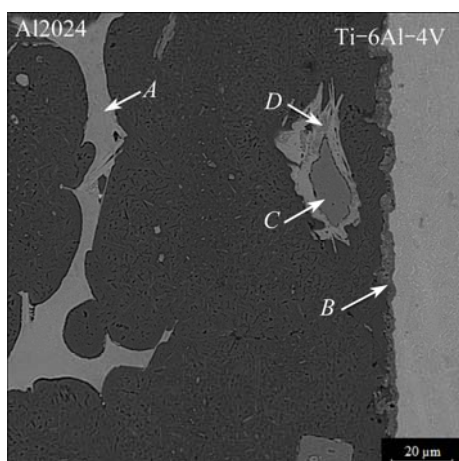


Fig. 2 SEM micrograph of bond made at 510 °C for 40 min

Table 3 EDS analysis of different areas in Fig. 2

Area	Mass fraction/%							
	Al	Cu	Zn	Ti	Mg	Mn	Fe	Si
<i>A</i>	45.48	49.92	0.03	0	0.27	0.96	3.33	0
<i>B</i>	47.32	42.34	0.39	9.05	0.18	0	0	0.72
<i>C</i>	69.75	6.02	0.74	0.12	0	9.95	13.42	0
<i>D</i>	47.96	37.97	0.33	0.30	0	5.11	8.26	0.08

With increasing bonding time up to 60 min, homogenization of the joint occurs and the process evolution is completed. As shown in Fig. 3(a), the joint zone made at bonding time of 60 min seems to be more uniform and a thin reaction layer forms at the interface. Furthermore, the sporadic phases in the interface vicinity are dissolved in comparison with that in the bond made at 40 min. In Fig. 3(b), the gradual diffusion of Cu and Zn forth of the joint zone is clarified by EDS analysis. It can be determined by weak peak intensities for Cu and

Zn at the bond interface. The presence of several elements such as Al, Cu, Zn, Mg, Si and Ti also suggests the formation of various intermetallic compounds at the interface.

Figure 4 illustrates EDS line scan of elements perpendicular to the interface for a bond made at 20 min.

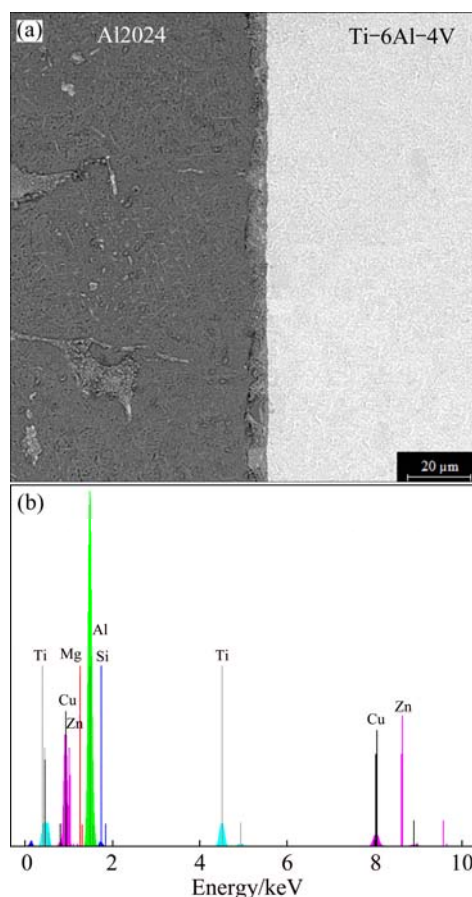


Fig. 3 SEM micrograph of bond made at 510 °C for 60 min (a) and EDS spectrum for interface region of joint made at 510 °C for 60 min (b)

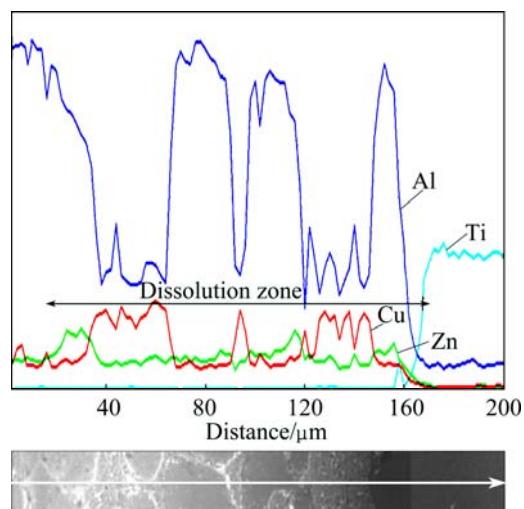


Fig. 4 EDS line scan of elements perpendicular to interface for bond made at 510 °C for 20 min

The width of dissolution zone and non-uniform distribution of elements in this zone are clearly observed. A severe decrease in Ti curve beside the dissolution zone has been seen, indicating negligible diffusion of Ti into the dissolution zone. Regarding short bonding time, finite diffusion of Cu and Zn in Ti alloy is evident. Despite severe Al peaks are located in dissolution zone, approving the existence of area *A* in Fig. 1, low peaks affirm the presence of areas *B* and *C*. Considering EDS line scan, the width of dissolution zone can be estimated to be 150  $\mu\text{m}$ .

Figure 5 indicates the distribution of composition for a bond made at 60 min. Uniform and complete diffusion of Cu and Zn into the parent metals is apparent in comparison with that of the bond made at 20 min. This indicates that with increasing bonding time, isothermal solidification and homogenization in the joint zone occur, so the joint width decreases to smaller than 10  $\mu\text{m}$ .

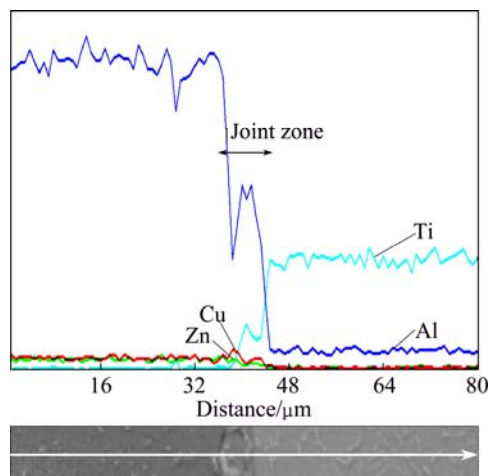


Fig. 5 EDS line scan of elements perpendicular to interface for bond made at 510 °C for 60 min

### 3.2 Identification of intermetallic compounds

In order to prove the formation of various intermetallic compounds in the joint zone, XRD analysis was applied. Figure 6 illustrates the XRD pattern of

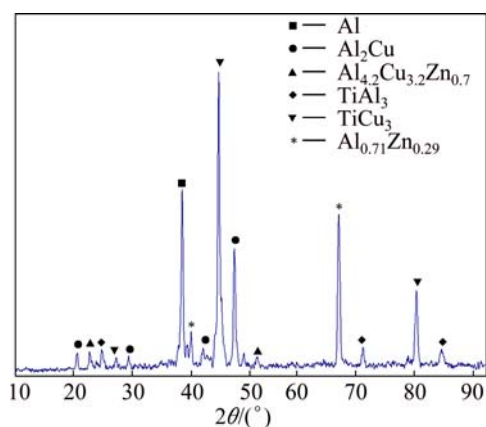


Fig. 6 XRD pattern of fractured Al alloy surface

fractured Al alloy surface. There are several peaks caused by the formation of intermetallics coupled with the peaks for aluminum which have been recognized as Al,  $\text{Al}_2\text{Cu}$ ,  $\text{Al}_{4.2}\text{Cu}_{3.2}\text{Zn}_{0.7}$ ,  $\text{TiAl}_3$ ,  $\text{TiCu}_3$  and  $\text{Al}_{0.71}\text{Zn}_{0.29}$ .

Figure 7 illustrates the XRD pattern obtained from fractured Ti alloy surface of the bond made at 60 min. The peaks for intermetallic compounds coupled with peaks for titanium which have been identified as Ti,  $\text{TiAl}_3$ ,  $\text{TiCu}_3$ ,  $\text{Ti}_2\text{Cu}$  and  $\text{TiZn}_{16}$ .

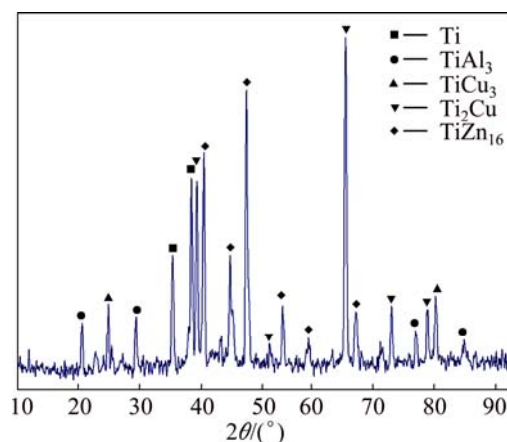


Fig. 7 XRD pattern of fractured Ti alloy surface

According to the XRD analysis, various intermetallic compounds form at the joint interface during the bonding process. Weak peak intensities are also observed for  $\text{TiAl}_3$  on the both fractured surfaces. In the solid-state diffusion bonding [4,11,12], because of direct contact of Ti and Al in the process and the higher bonding time compared with TLP bonding, the formation of various intermetallic compounds such as  $\text{TiAl}$ ,  $\text{TiAl}_3$  and  $\text{Ti}_3\text{Al}$  is expected, while in TLP bonding process, due to the presence of an interlayer between the base metals, the variety in the creation of these intermetallics is reduced and their contents at the interface are controlled.

### 3.3 Mechanical characterization of joints

Microhardness profiles of the joint zone for the bonds made at 20 and 60 min are shown in Fig. 8. The hardness value at the interface for a bond made at 20 min is VHN 118. With the increase in bonding time to 60 min, the hardness at the interface reaches VHN 153 due to the interdiffusion of Ti, Al, Cu and Zn and subsequently the formation of various intermetallic compounds. Moreover, the hardness value at two sides of the interface in the joint zone for the bond made at 60 min is noticeably higher than that of the bond made at 20 min. This indicates that with an increase in the bonding time, homogenization in the joint zone occurs and the joint width decreases.

Figure 9 represents shear strength of the bonds as a function of bonding time. Generally, with an increase in

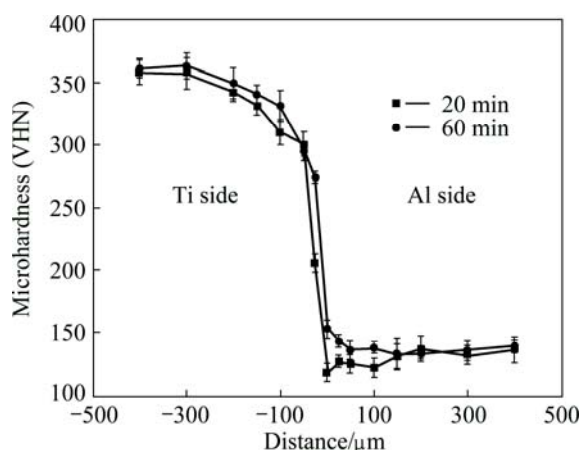


Fig. 8 Microhardness profiles of two bonds made at 510 °C for 20 and 60 min, respectively

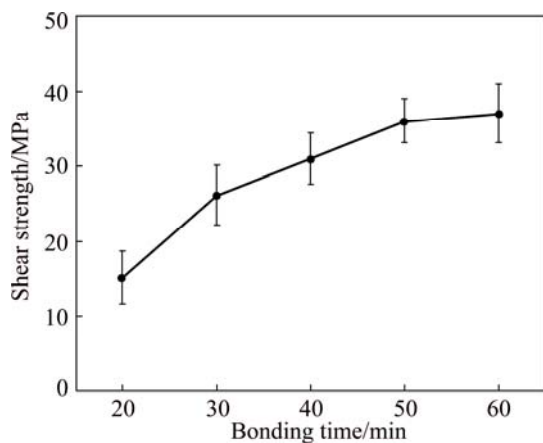


Fig. 9 Shear strength of bonds as function of bonding time

bonding time, shear strength of the joints made by Cu–Zn interlayer increases. This is attributed to the evolution of TLP process after 60 min and the formation of uniform intermetallic compounds at the interface. As it can be seen, the shear strength increasing rate at the first stages of TLP bonding process is high and then by increasing the bonding time it gradually decelerates in such a way that after 50 min, no significant changes occur in the joint strength. This could be attributed to the noticeable formation of  $\text{TiZn}_{16}$  at the interface demonstrated by XRD pattern (Fig. 7). This intermetallic compound identified by its brittleness have a detrimental effect on the mechanical properties of the joint [24]. In all samples, failure occurred across the bonded interface close to the Ti alloy. This indicates that solid-state diffusion bonding at the Ti alloy side is weaker than the TLP bonded part of the joint at Al alloy side. Nevertheless, the maximum shear strength of 37 MPa is obtained at 60 min. The maximum shear strength value recorded in this work is higher than the works that have used Cu and Sn–Zn–Bi interlayers to join Al alloy to Ti alloy [17,25].

## 4 Conclusions

Transient liquid phase bonding of Al 2024 to Ti–6Al–4V alloys by using Cu–22%Zn interlayer at 510 °C was performed. Creation of eutectic due to the diffusion of Cu and Zn within Al 2024 and solid-state diffusion bonding at Ti alloy side are responsible for the formation of metallurgical bond. Based on the XRD analyses, the presence of the interlayer between the alloys leads to the reduction of brittle intermetallics such as  $\text{TiAl}_3$  at the interface. By increasing the bonding time, the homogenization of the joint zone occurs and the joint width decreases to about 10  $\mu\text{m}$ . Furthermore, various intermetallic compounds like  $\text{Al}_2\text{Cu}$ ,  $\text{TiCu}_3$ ,  $\text{Ti}_2\text{Cu}$ ,  $\text{TiZn}_{16}$  and  $\text{Al}_{4.2}\text{Cu}_{3.2}\text{Zn}_{0.7}$  form at the interface. Regarding aforementioned reasons, the maximum shear strength reaches 37 MPa for the bond made at 60 min.

## References

- [1] HEINZ A, HASZLER A, KEIDEL C, MOLDENHAUER S, BENEDICTUS R, MILLER W S. Recent development in aluminium alloys for aerospace applications [J]. *Materials Science and Engineering A*, 2000, 280: 102–107.
- [2] MILLER W S, ZHUANG L, BOTTEMA J, WITTEBROOD A J, de SMET P, HASZLER A, VIIEGGE A. Recent development in aluminium alloys for the automotive industry [J]. *Materials Science and Engineering A*, 2000, 280: 37–49.
- [3] NUNES R. Properties and selection: Nonferrous alloys and special-purpose materials (Vol. 2) [M]. 10th ed. New York: ASM International, 1990.
- [4] FUKUTOMI H, NAKAMURA M, SUZUKI T, TAKAGI S, KIKUCHI S. Void formation by the reactive diffusion of titanium and aluminum foils [J]. *Materials Transactions—JIM*, 2000, 41: 1244–1246.
- [5] MA Zhi-peng, ZHAO Wei-wei, YAN Jiu-chun, LI Da-cheng. Interfacial reaction of intermetallic compounds of ultrasonic-assisted brazed joints between dissimilar alloys of Ti–6Al–4V and Al–4Cu–1Mg [J]. *Ultrasonics Sonochemistry*, 2011, 18: 1062–1067.
- [6] MA Zhi-peng, WANG Chang-wen, YU Han-chen, YAN Jiu-chun, SHEN Hao-ran. The microstructure and mechanical properties of fluxless gas tungsten arc welding–brazing joints made between titanium and aluminum alloys [J]. *Materials and Design*, 2013, 45: 72–79.
- [7] LÜ Shi-xiong, CUI Qing-long, HUANG Yong-xian, JING Xiao-jun. Influence of Zr addition on TIG welding–brazing of Ti–6Al–4V to Al5A06 [J]. *Materials Science and Engineering A*, 2013, 568: 150–154.
- [8] SONG Z H, NAKATA K, WU A P, LIAO J S. Interfacial microstructure and mechanical property of Ti6Al4V/A6061 dissimilar joint by direct laser brazing without filler metal and groove [J]. *Materials Science and Engineering A*, 2013, 560: 111–120.
- [9] CHEN Yan-bin, CHEN Shu-hai, LI Li-qun. Influence of interfacial reaction layer morphologies on crack initiation and propagation in Ti/Al joint by laser welding–brazing [J]. *Materials and Design*, 2010, 31: 227–233.
- [10] DRESSLER U, BIALLAS G, MERCADO U A. Friction stir welding of titanium alloy TiAl6V4 to aluminium alloy AA2024-T3 [J]. *Materials Science and Engineering A*, 2009, 526: 113–117.

- [11] REN Jiang-wei, LI Ya-jiang, FENG Tao. Microstructure characteristics in the interface zone of Ti/Al diffusion bonding [J]. *Materials Letters*, 2002, 56: 647–652.
- [12] YAO Wei, WU Ai-ping, ZOU Gui-sheng, REN Jia-lie. Formation process of the bonding joint in Ti/Al diffusion bonding [J]. *Materials Science and Engineering A*, 2008, 480: 456–463.
- [13] SOHN W H, BONG H H, HONG S H. Microstructure and bonding mechanism of Al/Ti bonded joint using Al–10Si–1Mg filler metal [J]. *Materials Science and Engineering A*, 2003, 355: 231–240.
- [14] KENEVISI M S, MOUSAVI KHOIE S M. Investigation on microstructure and mechanical properties of Al7075 to Ti–6Al–4V transient liquid phase (TLP) bonded joint [J]. *Materials and Design*, 2012, 38: 19–25.
- [15] LAVERNIA E J, GRANT N J. Aluminium–lithium alloys [J]. *Journal of Materials Science*, 1987, 22: 1521–1529.
- [16] COOK G O, SORENSEN C D. Overview of transient liquid phase and partial transient liquid phase bonding [J]. *Journal of Materials Science*, 2011, 46: 5305–5323.
- [17] ALHAZAA A, KHAN T I, HAQ I. Transient liquid phase (TLP) bonding of Al7075 to Ti–6Al–4V alloy [J]. *Materials Characterization*, 2010, 61: 312–317.
- [18] VOORT V, GEORGE F. *Metallography and microstructures* (Vol. 9) [M]. New York: ASM International, 2004.
- [19] ASTM standard D1002. Standard test method for apparent shear strength of single-lap-joint adhesively bonded metal specimens by tension loading (metal-to-metal) [S]. 1999.
- [20] ATIEH A M, KHAN T I. Application of Ni and Cu nanoparticles in transient liquid phase (TLP) bonding of Ti–6Al–4V and Mg–AZ31 alloys [J]. *Journal of Materials Science*, 2013, 48(19): 6737–6745.
- [21] ATIEH A M, KHAN T I. Transient liquid phase (TLP) brazing of Mg–AZ31 and Ti–6Al–4V using Ni and Cu sandwich foils [J]. *Journal of Science and Technology of Welding and Joining*, 2014, 19: 333–342.
- [22] RAGHAVAN V. Al–Cu–Zn (aluminum–copper–zinc) [J]. *Journal of Phase Equilibria and Diffusion*, 2007, 28: 183–188.
- [23] LIANG H, CHANG Y A. A thermodynamic description for the Al–Cu–Zn system [J]. *Journal of Phase Equilibria*, 1998, 19: 25–37.
- [24] GHOSH G, DELSANTE S, BORZONE G, ASTA M, FERRO R. Phase stability and cohesive properties of Ti–Zn intermetallics: First-principles calculations and experimental results [J]. *Acta Materialia*, 2006, 54: 4977–4997.
- [25] KENEVISI M S, MOUSAVI KHOIE S M. A study on the effect of bonding time on the properties of Al7075 to Ti–6Al–4V diffusion bonded joint [J]. *Materials Letters*, 2012, 76: 144–146.

## 用铜锌中间层瞬时液相连接 Al 2024 和 Ti–6Al–4V 合金

Majid SAMAVATIAN<sup>1</sup>, Ayoub HALVAEE<sup>2</sup>, Ahmad Ali AMADEH<sup>2</sup>, Alireza KHODABANDEH<sup>1</sup>

1. Department of Materials Engineering, Tehran Science and Research Branch,  
Islamic Azad University, Tehran 50122, Iran;

2. School of Metallurgy and Materials Engineering, University of Tehran, Tehran 50122, Iran

**摘要:** 采用 Cu–22%Zn 中间层, 在 510 °C、真空度为 0.01 Pa 和不同连接时间下将两种异质合金 Al 2024 和 Ti–6Al–4V 进行瞬时液相连接。采用 SEM、EDS 和 XRD 技术对连接区的显微组织演变进行表征。结果表明, 接头的形成归因于 Cu 和 Zn 固相扩散进入 Ti–6Al–4V 和 Al 2024 合金中, 然后形成共晶并沿 Cu–Zn/Al 2024 界面等温扩散。接头界面处的硬度随连接时间的延长而增加, 这是由于形成了 Al<sub>2</sub>Cu、TiCu<sub>3</sub>、Al<sub>4.2</sub>Cu<sub>3.2</sub>Zn<sub>0.7</sub>、Al<sub>0.71</sub>Zn<sub>0.29</sub>、Ti<sub>2</sub>Cu、TiAl<sub>3</sub> 和 TiZn<sub>16</sub> 金属间化合物。此外, 当连接时间为 60 min 时, 接头的剪切强度达到最大, 为 37 MPa。

**关键词:** 铝合金; 瞬时液相连接; 均匀化处理; 扩散; 金属间化合物; 共晶

(Edited by Wei-ping CHEN)